Growth of carbon nanotubes by gas source molecular beam epitaxy

J. Wan,[a] Y. H. Luo, Sung D. Choi, R. G. Li, G. Jin, J. L. Liu, and K. L. Wang
Device Research Laboratory, Electrical Engineering Department, University of California at Los Angeles, Los Angeles, California 90095-1594

(Received 27 June 2000; accepted for publication 7 November 2000)

Multiwall carbon nanotubes have been grown by gas source molecular beam epitaxy in the presence of Ni catalyst. Some nanotubes show thinner bases compared with their heads. First- and second-order Raman scattering spectra are used to study the structure of samples with different initial thicknesses of Ni layers. The second-order $2D$ Raman mode of carbon nanotubes shows a downshift compared with the graphite-like structure. The growth of carbon nanotubes is found to depend on the size of the metal droplets. When the initial Ni layer is either too thick or too thin, few carbon nanotubes are observed. The Raman spectra show graphite and glassy carbon structures for too thick and too thin initial Ni layer films, respectively. Only when a proper range of Ni catalyst film is used, carbon nanotubes could be found. © *2001 American Institute of Physics.*
[DOI: 10.1063/1.1337083]

I. INTRODUCTION

In 1991, the discovery of multiwall carbon nanotubes was first reported.[1] A few years later, single wall carbon nanotubes were also observed.[2] Due to their potential applications in electronic devices, nanotechnology tools, and high-performance nanoscale materials,[3,4] carbon nanotubes have been widely studied theoretically and experimentally. At present, carbon nanotubes can be synthesized by arc discharge,[1,5] laser ablation,[6] pyrolysis of hydrocarbons,[7] chemical vapor deposition (CVD),[8–10] ion beam irradiation,[11] and scanning tunneling microscope.[12] It was also reported that carbon nanotubes could be grown from carbon vapor under ultrahigh vacuum conditions without the presence of a catalyst.[13] The growth mechanisms of carbon nanotubes using these methods were different and complicated. Compared with these methods, molecular beam epitaxy (MBE) is an easy growth process and offers powerful tools, such as reflected high energy electron diffraction, Auger electron spectroscopy, etc., for *in situ* study of the growth mechanism. Previously we have grown Si whiskers on a Au/Si(111) substrate using this method.[14] In this article, the growth of carbon nanotubes by gas source MBE with the presence of a Ni catalyst is reported.

II. EXPERIMENTS

(100) *p*-Si substrates were thermal oxidized to have a 100 nm thick SiO_2 layer. A Ni layer of 1–15 nm thickness was then deposited on the substrate via e-beam evaporation in a vacuum of 10^{-6} Torr at room temperature. Subsequently, the substrate was introduced into a gas source MBE chamber. Carbon nanotube growth was performed by introducing pure C_2H_2 gas at a pressure of 3×10^{-5} Torr with the substrate temperature held at 750 °C. The growth time was about 2 h.

[a]Electronic mail: jwan@ee.ucla.edu

III. RESULTS AND DISCUSSION

Figure 1(a) shows a low-magnification scanning electron microscopy (SEM) image of carbon nanotubes grown on a substrate with a 5 nm Ni layer at 750 °C. The nanotubes had lengths of 300–700 nm and diameters of about 30–50 nm. Because of their larger diameters and the Raman spectra, which will be discussed later, they are multiwall nanotubes. The areal density of the nanotubes was $2-3\times10^{8}$ cm^{-2}. Figure 1(b) shows a SEM image with higher resolution. The base of a nanotube located at a hole, indicated by arrow ''A'' in Fig. 1(b), and the top of the nanotube were capped with a Ni nanoparticle (indicated by arrow ''B''). It should be noted that some nanotubes had thinner bases than heads, as indicated by arrow ''C,'' the reason for which needs further study. Figures 1(c) and 1(d) are SEM images of the nanotubes grown on a substrate with a 15 nm thick Ni layer. Compared with Figs. 1(a) and 1(b), the density of the nanotubes is lower and the diameter of the nanotube is larger (about 100 nm). For the sample grown on a 1 nm Ni layer, almost no carbon nanotubes were observed (not shown here). This means that the growth of nanotubes is influenced by the initial thickness of the Ni layer. For growth of carbon nanotubes by CVD using catalyst particles, both base-growth and tip-growth modes appear to be possible.[8] In the base-growth mode, the carbon nanotubes were formed by extrusion, resulting in a closed top end. In contrast, in the tip-growth mode, a metal catalyst particle remained on top of each nanotube during growth. In our MBE method, the growth of carbon nanotubes seemed to be tip-growth mode, since the Ni droplets were observed to be on the tops of the carbon nanotubes, as seen in Figs. 1(b) and 1(d). In this mode, C_2H_2 gas molecules were absorbed on the metal droplets and dissolved into carbon atoms, then dissolved carbon atoms aggregated and formed into nanotubes. During growth, the metal domain was pushed upwards by the carbon nanotube

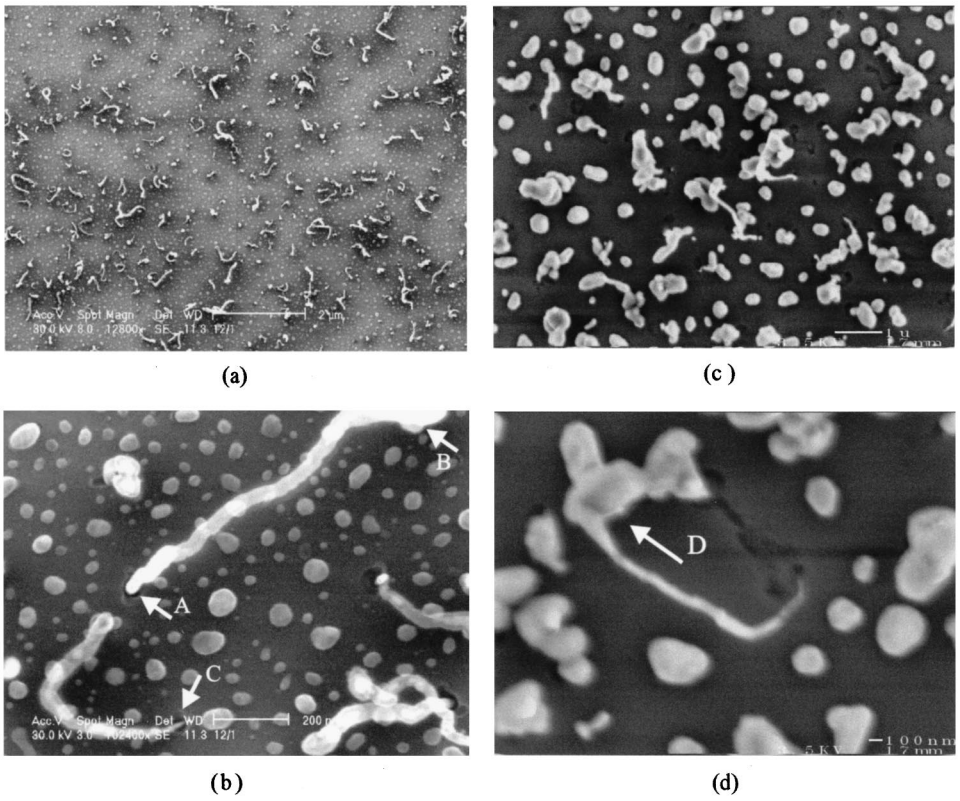

FIG. 1. SEM images of samples grown by MBE at 750 °C for 2 h on Ni layers with different thicknesses. (a) Low-magnification and (b) high-magnification images of carbon nanotubes grown on a 5 nm thick Ni layer substrate. Arrows ''A'' and ''B'' are the base and tip of carbon nanotubes, respectively. The base of one nanotube was much thinner than the bulk, as indicated by arrow ''C.'' (c), (d) Low- and high-magnification images of the sample grown on a 15 nm Ni substrate. The top of the nanotubes is bigger, as indicated by arrow ''D.''

and formed a metal cap on the top of the nanotube. Therefore, the growth of carbon nanotubes was certainly influenced by the size of the metal droplets.

Figure 2 shows atomic force microscopy images of the substrates after Ni metal layer deposition and annealing at 750 °C for 10 min in the growth chamber (before C_2H_2 introduction). The images in Figs. 2(a)–2(d) correspond to 1, 3, 5, and 15 nm thick Ni layers, respectively. The heat treatment changes the smooth Ni films into Ni droplets on the SiO_2 surface. The droplets of Ni are semispherical particles. From the AFM images, it is seen that 750 °C is a sufficiently high temperature to get droplet formation of Ni particles; and it is consistent with Ref. 9, in which it was reported that Ni films were transformed into Ni droplets by heat treatment at 700 °C. For the 1 nm thick Ni layer [Fig. 2(a)], the diameters of droplets were 15–20 nm. As the thickness of the Ni layer increased, the diameter of the droplets increased. For the 5 nm thick Ni layer [Fig. 2(c)], the droplets showed the most uniformity with diameters of 100–200 nm, so the density of carbon nanotubes on this substrate was highest, as shown in Fig. 1(a). When the thickness of the Ni layer was increased to 15 nm [Fig. 2(d)], the Ni droplets became much larger and nonuniform even with the diameter increased to 500 nm. Fewer carbon nanotubes were observed, as shown in Fig. 1(c). The dependence of the initial Ni layer thickness on the growth of carbon nanotubes was consistent with previous CVD results, where the carbon nanotubes could grow only from Ni droplets with specific diameters.[9]

Raman spectroscopy has been recognized as one of the most sensitive methods with which to study the structural properties of carbonaceous materials. The Raman measurements were performed at room temperature, using the 514.5 nm line of an Ar^+ laser as the excitation source. Figure 3(a) shows the first-order Raman spectra of the deposits on Ni films with different initial thicknesses. Without the deposited Ni layer, no carbon-related Raman peak was observed, as seen in Fig. 3(a), which indicates the importance of the Ni layer as a catalyst. For the 1 nm thick Ni layer sample, two

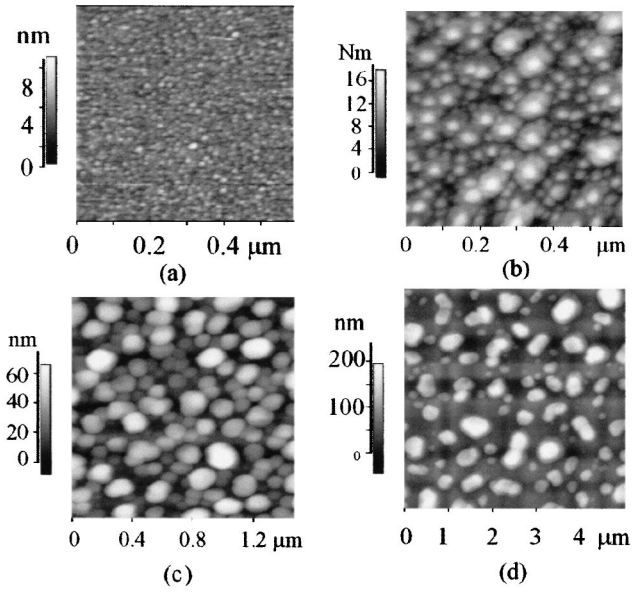

FIG. 2. Atomic force microscopy images of the annealed substrates with various Ni layer thicknesses at 750 °C for 10 min. Images (a)–(d) correspond to substrates with 1, 3, 5, and 15 nm Ni layer thicknesses, respectively. The 5 nm Ni sample shows droplets of quite uniform size after annealing.

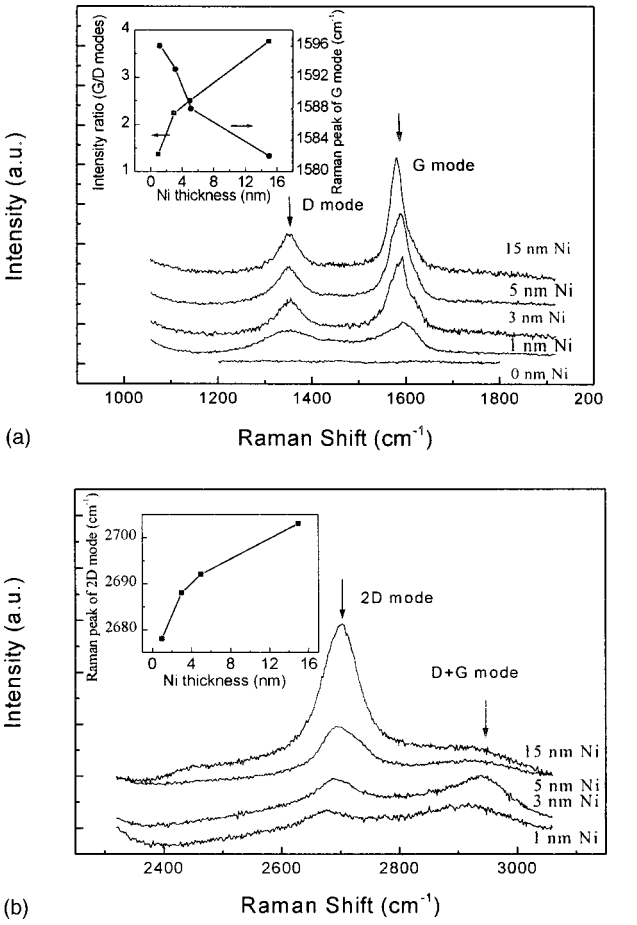

FIG. 3. (a) First-order and (b) second-order Raman spectra of samples grown by MBE at 750 °C for 2 h. The intensity ratio between the *D* and *G* modes and the Raman shifts of the *G* mode are shown in the inset of (a). The Raman shift of the 2*D* mode is shown in the inset of (b). For the 5 nm Ni sample, the 2*D* mode showed an obvious downshift compared with that of a graphite-like structure.

peaks located at 1352 and 1596 cm^{-1} were observed, showing a typical Raman spectrum of the glassy carbon.[15,16] The peak around 1352 cm^{-1}, known as the *D* mode, was explained in terms of the relaxation of the wave vector selection rules in solid carbon, resulting from the finite crystal size, which allowed the *M* point phonon to contribute to Raman scattering.[15] The 1596 cm^{-1} peak is called the *G* mode, which was assigned to the vibrational mode corresponding to movement in the opposite direction of two neighboring carbon atoms in a graphite sheet.[15] When the thickness of the initial Ni layer and therefore the size of the Ni droplets increased, as for the cases shown in Figs. 2(b)–2(d), the intensity ratio between the *G* mode peak and the *D* mode peak increased. This indicated that the deposited carbon related materials became more and more crystalline when the size of the Ni droplets increased, since the *D* mode peak is in terms of relaxation of the wave vector selection rules in solid carbon. At the same time, the *G* mode showed a downshift with an increase of the initial Ni layer thickness. When the thickness of the Ni layer was increased to 15 nm, the 1596 cm^{-1} peak shifted to 1582 cm^{-1}, which is the value of graphite. Considering the nanotube diameters observed in Fig. 1, the *G* mode peak is close to its value in graphite of larger diameter (15 nm thick Ni layer, 100 nm diam nanotube, 1582 cm^{-1}) and is higher for a smaller diameter (5 nm thick Ni layer, 30–50 nm diam nanotube, 1588 cm^{-1}). Except for the *D* and *G* modes, the distinctive Raman mode for nanotubes is the radial mode spectra. We attempted to characterize the radial mode of the samples. However, no distinguishing peak is observed. According to Jantoljak *et al.*,[5] the intensity ratio of the radial mode to the *G* mode is about 1:50 for purified multiwall nanotubes. As the areal density of nanotubes on our sample is not high enough and the nanotubes are not purified, it is understandable that the radial mode is not observed.

Compared with the first-order Raman spectra, the second-order Raman spectra also gave a wealth of information on the formation of carbon nanotubes. The second-order Raman spectra of our samples are shown in Fig. 3(b). For the 1 nm thick Ni layer sample, two peaks located at 2678 and 2920 cm^{-1} were observed. The 2678 cm^{-1} peak is believed to downshift from the peak at $2\times1352\,\mathrm{cm}^{-1}=2704\,\mathrm{cm}^{-1}$, which was denoted as the 2*D* mode. The 2920 cm^{-1} peak was close to $1352+1581\,\mathrm{cm}^{-1}=2933\,\mathrm{cm}^{-1}$, which was assigned to the $D+G$ mode. This combination peak $(D+G)$ represents the sum of two phonons with two unequal energies while the overtone peak $(2D)$ was from two phonons belonging to the same branch of the phonon dispersion curves. In general, because of the wave vector conservation, the Raman intensity of the overtone peak $(2D)$ should be stronger than that of the combination peak. However, it is not the case for the 1 nm thick Ni layer samples, in which the $D+G$ peak is stronger than the 2*D* peak. The reason might be that the carbon structure grown on the 1 nm Ni layer was a glass-like structure, as confirmed by the first-order Raman spectrum in Fig. 3(a). In the glassy or microcrystalline carbon, the wave vector conservation restriction was relaxed,[17] and the peak of the $(D+G)$ mode could be observed more easily. For the Ni layer 15 nm thick, the position of the 2*D* mode was at 2703 cm^{-1}, which is very close to $2\times1352\,\mathrm{cm}^{-1}=2704\,\mathrm{cm}^{-1}$. The $D+G$ peak intensity was rather low and this Raman spectrum was much like that of graphite.[15,16] For the case with the 5 nm thick Ni layer, i.e., between the above two extremes, the 2*D* peak showed up at 2692 cm^{-1} and had an 11 cm^{-1} downshift compared with that of the 15 nm thick Ni layer sample; also, the 2*D* peak was much stronger than the $D+G$ mode. In this case, many carbon nanotubes were observed, as seen in Fig. 1(a). In Ref. 16, the 2*D* mode of nanotubes with a diameter of 30 nm showed an ~25 cm^{-1} downshift compared with those of highly oriented pyrolytic graphite,[15,16] therefore, the downshift or 2*D* mode in our sample is consistent with the former results.

IV. CONCLUSION

Multiwall carbon nanotubes were grown by gas source MBE and studied by SEM and Raman spectroscopy. The growth mechanism of nanotubes was attributed to the tip-growth mode. The yield of carbon nanotubes was found to be

dependent on the size of the metal catalyst droplets. The diameter of nanotubes increases with the thickness of the initial thickness of Ni layer.

ACKNOWLEDGMENTS

The authors acknowledge partial support by the Semiconductor Research Corporation and by the National Science Foundation.

[1] S. Iijima, Nature (London) **354**, 56 (1991).
[2] S. Iijima and T. Ichihashi, Nature (London) **363**, 603 (1993).
[3] P. G. Collins, A. Zettl, H. Bando, A. Thess, and R. E. Smalley, Science **278**, 100 (1997).
[4] H. Dai, J. H. Hafner, A. G. Rinzler, D. T. Colbert, and R. E. Smalley, Nature (London) **384**, 147 (1996).
[5] H. Jantoljak, J.-P. Salvetat, L. Forro, and C. Thomsen, Appl. Phys. A: Mater. Sci. Process. **67**, 113 (1998).
[6] A. Thess *et al.*, Science **273**, 483 (1996).
[7] H. M. Cheng, F. Li, G. Su, H. Y. Pan, L. L. He, X. Sun, and M. S. Dresselhaus, Appl. Phys. Lett. **72**, 3282 (1998).
[8] Y. Gao, J. Liu, M. Shi, S. H. Elder, and J. W. Virden, Appl. Phys. Lett. **74**, 3642 (1999).
[9] M. Yudasaka, R. Kikuchi, T. Matsui, Y. Ohki, S. Yoshimura, and E. Ota, Appl. Phys. Lett. **67**, 2477 (1995).
[10] Z. F. Ren, Z. P. Huang, J. W. Xu, J. H. Wang, P. Bush, M. P. Siegal, and P. N. Provencio, Science **282**, 1105 (1998).
[11] K. Yamamoto, Y. Koga, S. Fujiwara, and M. Kubota, Appl. Phys. Lett. **69**, 4174 (1996).
[12] J. Yamashita, H. Hirayama, Y. Ohshima, and K. Takayanagi, Appl. Phys. Lett. **74**, 2450 (1999).
[13] M. Ge and K. Sattler, Science **260**, 515 (1993).
[14] J. L. Liu, S. J. Cai, G. L. Jin, S. G. Thomas, and K. L. Wang, J. Cryst. Growth **200**, 106 (1999).
[15] H. Hiura, T. W. Ebbesen, K. Tanigaki, and H. Takahashi, Chem. Phys. Lett. **202**, 509 (1993).
[16] J. Kastner, T. Pichler, H. Kuzmany, S. Curran, W. Blau, D. N. Weldon, M. Delamesiere, S. Draper, and H. Zandbergen, Chem. Phys. Lett. **221**, 53 (1994).
[17] R. J. Nemanich and S. A. Solin, Phys. Rev. B **20**, 392 (1979).